19. Paranjpe, A. S. and Gokhale, G. K., Pharmacological study of embelin with reference to its use as an anthelmintic. *Arch. Inst. Pharmacodyn.*, 1932, **42**, 212.
20. Agrawal, S., Chauhan, S. and Mathur, R., Antifertility effects of embelin in male rats. *Andrologia*, 1986, **18**(2), 125–131.
21. Radhakrishnan, N., Gnanamani, A. and Mandal, A. B., A potential antibacterial agent embelin, a natural benzoquinone extracted from *Embelia ribes*. *Biol. Med*., 2011, **3**(2), 1–7.
22. Simpkin, K. G. and Coles, G. C., The use of *Caenorhabditis elegans* for anthelmintic screening. *J. Chem. Technol. Biotechnol*., 1981, **31**, 66–69.
23. Ganesan, B., Perumal, P., Manickam, V. B., Gotteti, S. D., Srikakolapu, S. R. and Thirumurthy, L. S., Optimization of extraction conditions for embelin in *Embelia ribes* by UV spectrophotometry. *Arch. Appl. Sci. Res*., 2010, **2**(2), 49–53.
24. Hope, I. A., *C. elegans: A Practical Approach*, Oxford University Press, Oxford, New York, 1999, p. 281.
25. Jesudason, M. V., Balaji, V. and Densibai, S., Toxigenicity testing of clinical isolates of non-typhoidal salmonellae in Vero cell culture and *Caenorhabditis elegans* model. *Indian J. Med. Res*., 2006, **123**(6), 821–824.
26. Venkatasubramanian, P., Kumar, S. K. and Nair, V. S., *Cyperus rotundus*, a substitute for *Aconitum heterophyllum*: studies on the Ayurvedic concept of Abhava Pratinidhi Dravya (drug substitution). *J. Ayurveda Integr. Med.*, 2010, **1**(1), 33–39.
27. Eguale, T., Tilahun, G., Debella, A., Feleke, A. and Makonnen, E., *In vitro* and *in vivo* anthelmintic activity of crude extracts of *Coriandrum sativum* against *Haemonchus contortus*. *J. Ethnopharmacol*., 2007, **110**(3), 428–433.
28. Stermitz, F. R., Lorenz, P., Tawara, J. N., Zenewicz, L. A. and Lewis, K., Synergy in a medicinal plant: antimicrobial action of berberine potentiated by 5′-methoxyhydnocarpin, a multidrug pump inhibitor. *Proc. Natl. Acad. Sci. USA*, 2000, **97**(4), 1433–1437.
29. Rasoanaivo, P., Wright, C. W., Willcox, M. L. and Gilbert, B., Whole plant extracts versus single compounds for the treatment of malaria: synergy and positive interactions. *Malaria J.* (*Suppl. 1*), 2011, **10**, S4.
30. Martin, R. J., Modes of action of anthelmintic drugs. *Vet. J*., 1997, **154**(1), 11–34.

ACKNOWLEDGEMENTS. We thank Dr Sandhya Koushika (TIFR, Mumbai) for providing wild type (Bristol N2) *C. elegans* strain and training in *C. elegans* culture techniques; Prof. Nagarajan (IAIM, Bangalore), Ojal and Lubna for their valuable suggestions and help during the experiments; Karthikeyan for help in statistical analysis and Dr Ravikumar and Dr Goraya for procurement and authentication of plant species. This work was supported by funding from Ministry of Environment and Forests, Govt of India, and DST-Drugs and Pharmaceuticals Research Program, Govt of India.

Received 8 February 2013; revised accepted 8 October 2013

Reliability of earthquake nucleation model in Koyna region

S. S. Rai[1] and Rajgopala Sarma[2,*]

[1]CSIR-National Geophysical Research Institute, Uppal Road, Hyderabad 500 007, India
[2]LIG 989, KPHB Colony, Hyderabad 500 072, India

We question the inferred downward nucleation of hypocentres that forms the basis for short-term earthquake prediction in the Koyna region. A careful relocation of foreshocks/aftershocks for a *Mw* 4.4 main shock sequence in 1996, hitherto believed to have occurred at 8 km depth, reveals that the main shock occurred at a depth of only 1.8 km, and formed part of a clear and almost instantaneous northward migration of micro-earthquakes along a narrow zone that could only be a fault plane at 4–8 km depth. This finding requires the current hypothesis for forecasting deep main shocks from shallow foreshocks in Koyna region to be discarded.

Keywords: Earthquake nucleation, micro-earthquakes, short-term prediction.

THE study of the earthquake nucleation process is one of the important problems in earthquake mechanics. While the precise earthquake prediction is a distant dream, efforts have been made towards short-term prediction using diagnostic features of earthquake patterns occurring before the main shock. The concept emerged from laboratory experiments that suggest 'during the nucleation, the energy is exclusively consumed in and around nucleation zone… Accordingly, dynamic instabilities of small scales (micro-seismicity) are induced and activated during the nucleation process… The model shows that immediate foreshock activity is a part of main shock earthquake nucleation…'[1]. This concept along with continuous downward depth migration of earthquakes prior to the main shock occurrence has been patented and used as a model for short-term earthquake prediction in Koyna region[2,3]. The results suggest that fracture nucleates at shallow depth (<1 km) and gradually deepens to cause the main shock at a depth of 8–11 km.

The above result of depth migration from shallow to deeper level is at variance with the well-known physical basis that due to the progressive homogenization of the crust with depth, the rupture that nucleates in the shallower region is inhibited from propagating due to presence of small inhomogeneities, while those nucleating in deeper regions (high stress drop) have the probability of growing into a main shock and propagate over the entire fault plane[4,5]. We study here the validity of the proposed nucleation model presented for Koyna region earthquakes

*For correspondence. (e-mail: rajgopalasame@gmail.com)

using one of the small earthquake sequences recorded by us during 1996.

The sequence (22/4/1996 to 29/4/1996) includes 150 micro-earthquakes (mag > 1.5) and a $Mw = 4.4$ main shock (Figure 1). We show that foreshocks and aftershocks propagate northwards along a fault plane largely confined to a depth range 4–8 km, and that the main shock occurs at ~1.8 km depth.

We now describe the steps undertaken to ensure the precise location of earthquake hypocentres. Our data included earthquake waveforms recorded at 100 samples/s by the Koyna digital seismic network comprising triaxial 1 Hz sensors and REFTEK 72A-07 data acquisition system with GPS time-tagging. Details of the experiment are presented by Rai *et al.*[6].

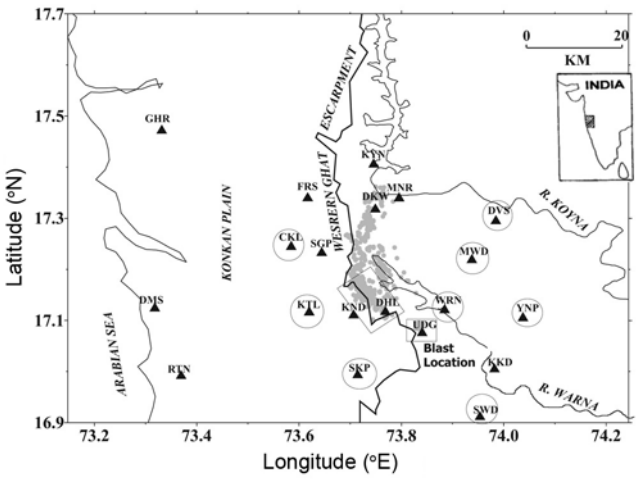

Figure 1. Major geological features and seismicity pattern of Koyna seismic zone observed during 1996–98 (shown by grey dots). Triangle denotes the seismograph locations. The earthquake sequence (22–29 April 1996) used for analysis is shown by rectangle around stations KND and DHL. These earthquakes were recorded by eight seismographs shown by circles. Blast location is shown by a square around UDG.

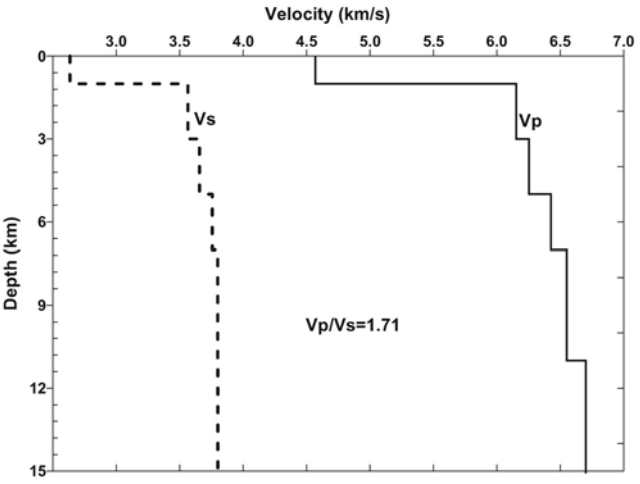

Figure 2. Reference 1D *P* and *S* velocity model used to locate earthquakes.

Accurate location is a pre-requisite for any meaningful study of the mechanics of foreshocks. This requires an appropriate velocity model and sufficient number of *P* and *S* phase arrival time data to obtain well-constrained hypocentre estimates. The 1D reference velocity model was obtained from a larger dataset from digital seismic network in Koyna region[6] using VELEST earthquake location program[7]. The resulting velocity model (Figure 2) was used to locate the earthquake sequence. To establish the reliability of earthquake hypocentre, we first calibrated our location methodology considering a number of chemical explosions used for bauxite mining in the study zone in a 2×2 sq. km area around 17°5.05′N and 73°49.90′E (Figure 1). These explosions were treated as earthquakes for the purpose. Only *P* arrival times were used to locate these explosions. The computed epicentre locations and focal depths for chemical explosions are presented in Figure 3. On comparing the observed and computed hypocentres we conclude that epicentre error is generally less than 0.5 km and focal depth error is less than 1.5 km (for 80% of explosions). The above error estimates probably represent the upper bound because (i) the explosions are located in one extreme corner of the network with a large azimuthal gap (generally more than 180°), (ii) they are surface focus (< 50 m) and (iii) only *P*-phase data are used.

We expect much smaller error in hypocentre estimates for a typical earthquake at depth compared to explosions. From a sequence of 150 earthquakes, we selected 85 events each with at least 6*P* and 4*S* phase readings, to study hypocentre location reliability. Epicentre location and the histogram of earthquake depth distribution, error statistics for the time residual (rms), horizontal distance error (erh) and depth error (erz) are presented in Figure 4. Note that erh and erz depict only convergence error in epicentre and focal depth, rather than the location errors, because, they represent hypocentral adjustment for a new computation to be performed. Examination of the error statistics reveals that ~85% of event have rms <0.08 sec, erh <0.6 km and erz <1.5 km. These numbers clearly demonstrate the high quality of data and the hypocentral location of the earthquake sequence. The sequence is confined to 2×2 sq. km area with the maximum event concentration in 4–8 km depth range. The maximum focal depth is 10 km. The depth pattern of this sequence is similar to that derived for the entire seismic zone from a larger dataset[6].

Earthquake hypocentres were further improved by relocating the above earthquake sequence using hypoDD algorithm[8,9], which exploits similarities in the event–station paths of a closely spaced cluster of events recorded at a relatively farther distance. In such a case, the difference in travel times from two earthquakes recorded at a station can be attributed to spatial offset between the events[10]. The algorithm has the advantage of minimizing the error due to unmodelled intervening

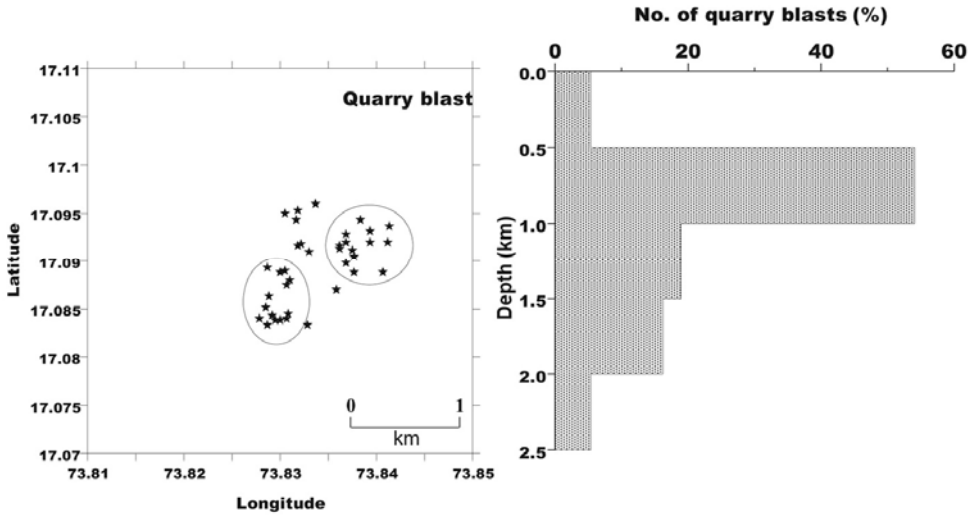

Figure 3. Location and depth distribution of chemical explosions. Mining area is shown by ellipse.

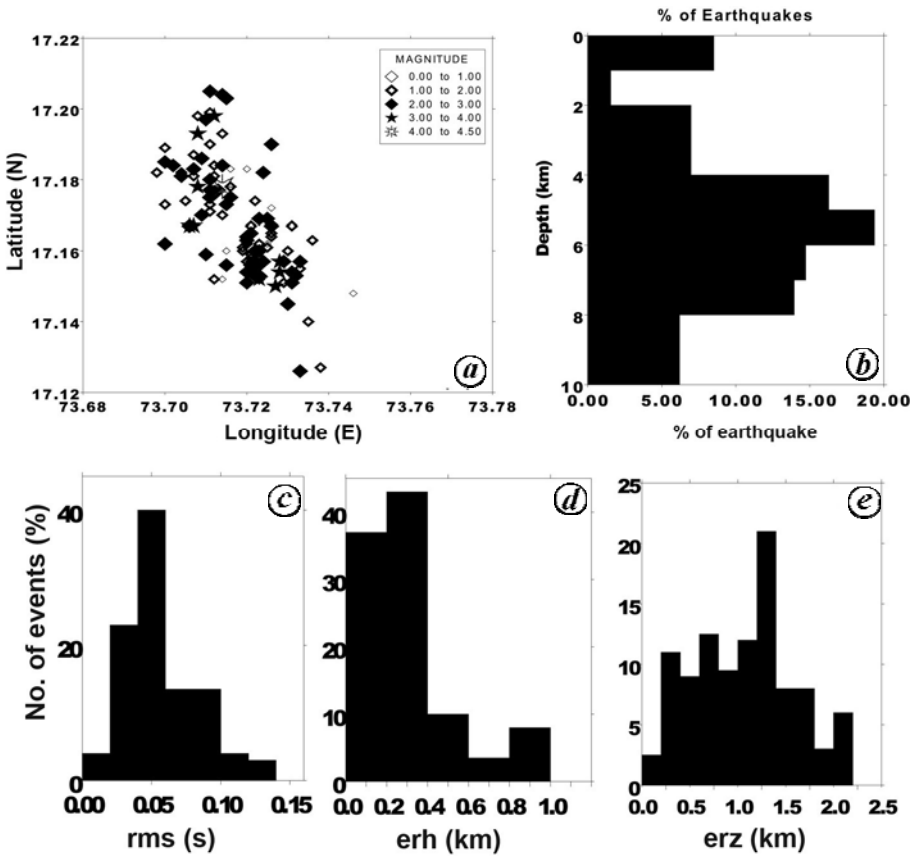

Figure 4. ***a***, Epicentre distribution of earthquakes; ***b***–***e***, Histograms of earthquake: ***b***, Depth distribution; ***c***, Time residual (sec); ***d***, Error in epicentral distance (km); ***e***, Error in focal depth (km).

inhomogeneities of comparable larger size, without the need for station correction. The travel times for *P* and *S* phases were provided from earlier located datasets using the VELEST. The earthquake data catalogue was examined for event pairs with phase arrival at common stations. Since the earthquakes here are in a small region, all of them were grouped in a single cluster. This led to minimal loss of data during relocation. We minimized the double-difference residual using conjugate gradient method[11]. We followed the double-difference approach to relocate both the mining blasts and also the earthquakes. Details of error in longitude, latitude and focal

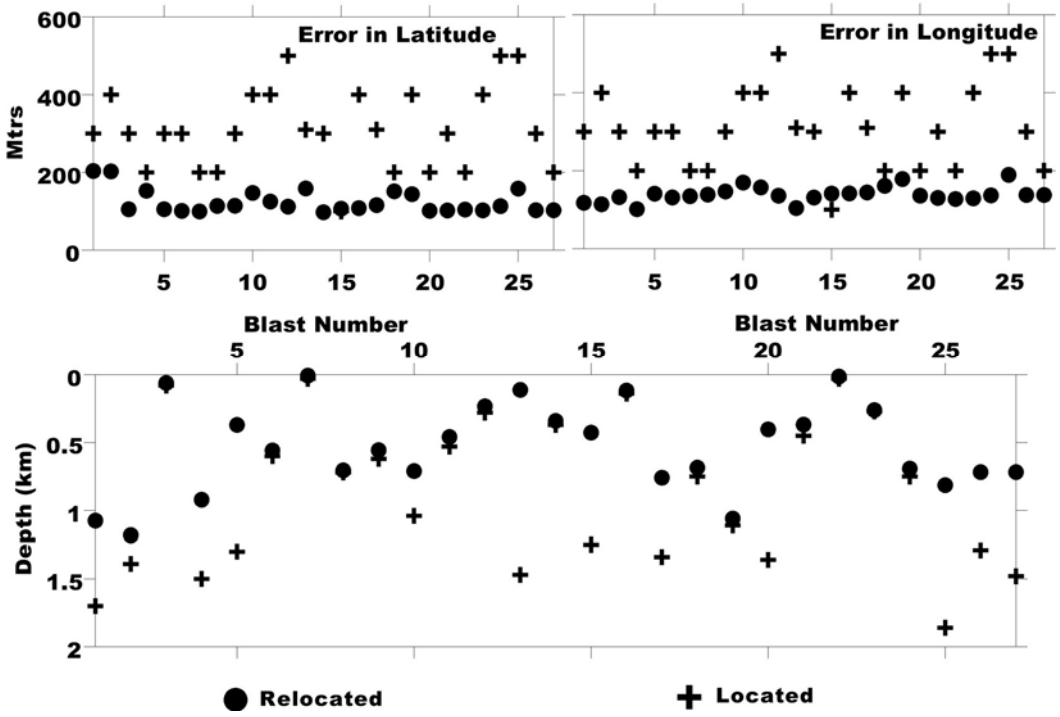

Figure 5. Comparison of error in latitude, longitude and focal depth for chemical explosions using the initial single-event and final double-difference locations.

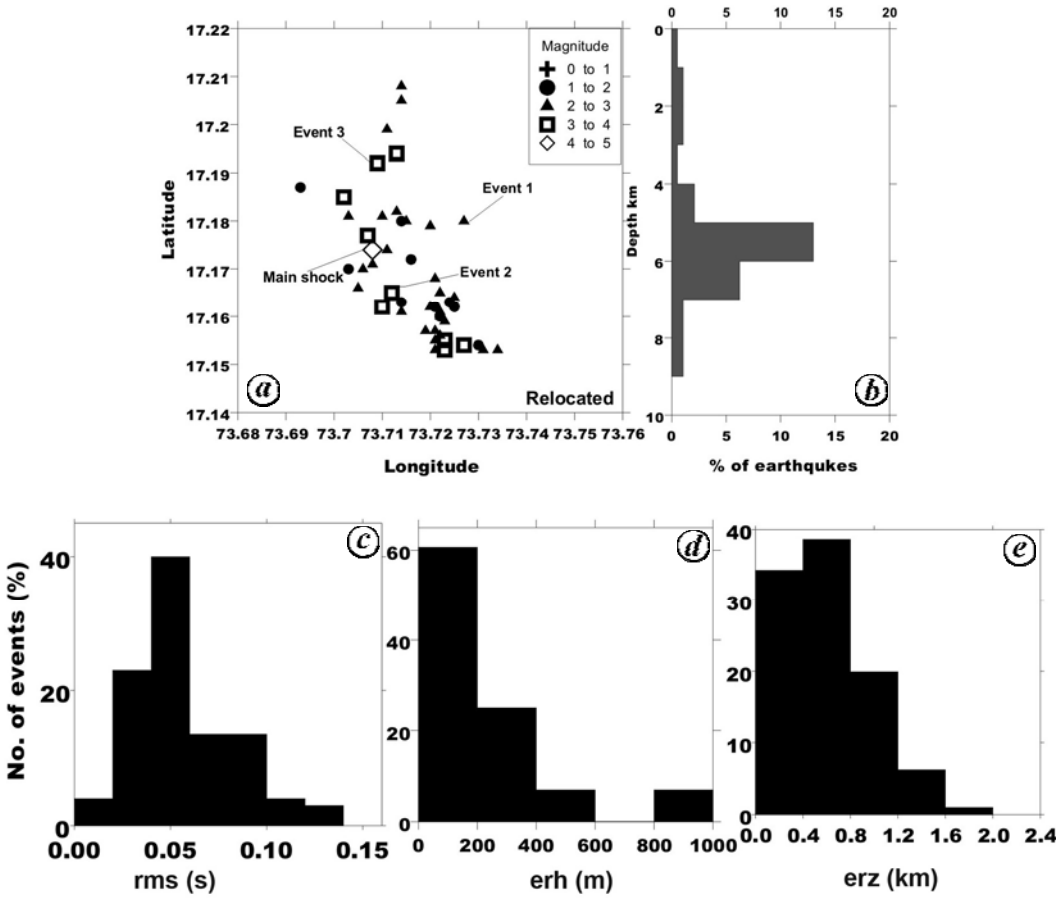

Figure 6. (***a***) Relocated earthquake epicenter; (***b***) Earthquake depth histogram; (***c***) Histogram of rms error; (***d***) error in epicentre; (***e***) Depth estimate using HypoDD.

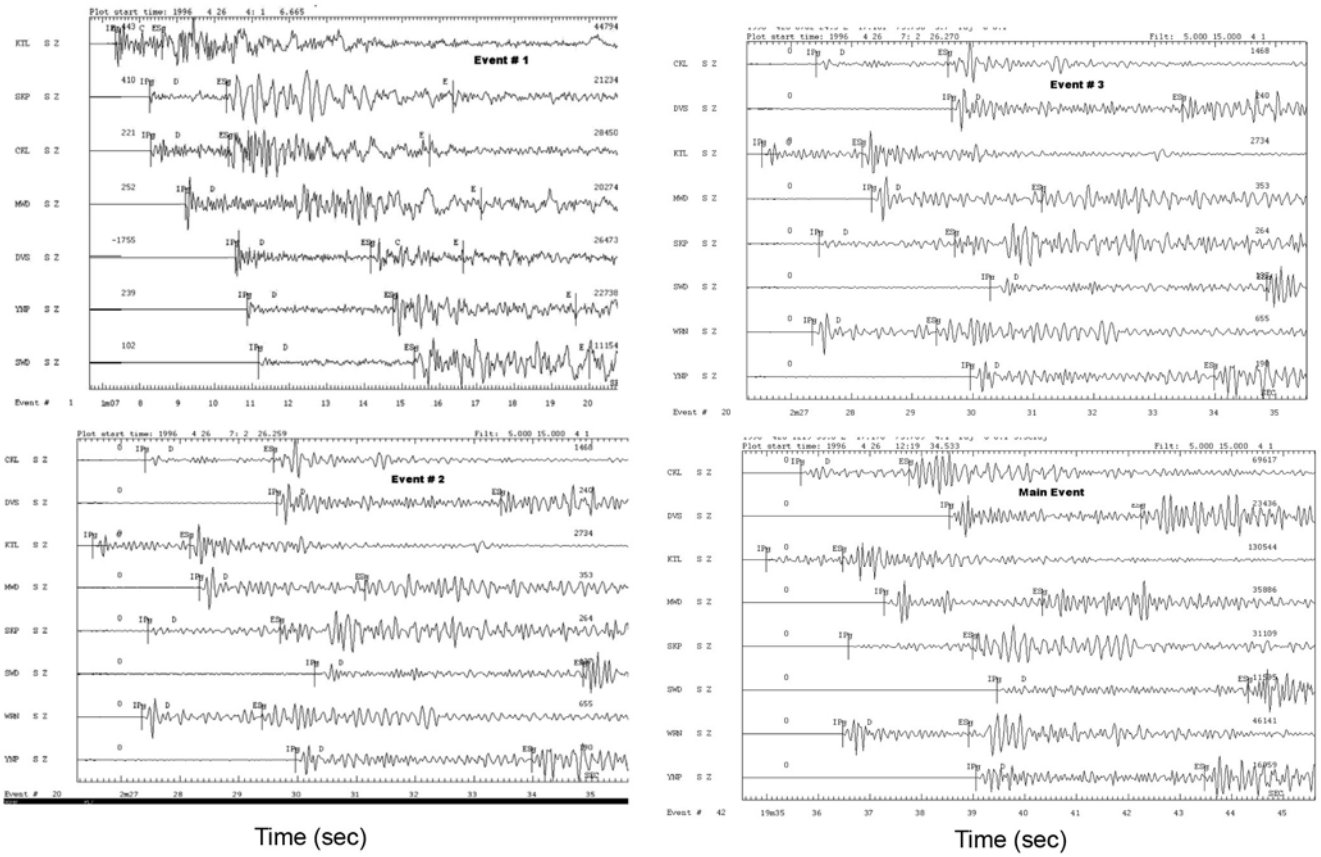

Figure 7. Vertical component recordings of seismograms for four earthquakes used to re-estimate the depth.

depth for both the initial and relocated datasets for explosion data are presented in Figure 5. Results show significant improvement in all the relocated parameters for explosion data, for example, average epicentre and depth error is reduced to ~100 and ~600 m respectively. These are the benchmark for actual error expected in hypocentre location of earthquakes. Figure 6 shows spatial distribution of earthquakes, their depth pattern and histogram of error in time (rms), erh and erz. These errors are significantly less compared to initial single-event locations (shown in Figure 4). Over 90% of events have epicentre and depth error of less than 600 and 1500 m respectively.

To further establish reliability of earthquake focal depth obtained through inversion of travel-time data, we selected four earthquakes (marked as events 1, 2, 3 and main shock in Figure 6 *a*) and performed a series of inversions for earthquake location with only three free parameters (latitude, longitude and origin time), whereas depth was held fixed each time. This was performed for a number of pre-selected focal depths at discrete intervals. Waveform of these events recorded at selected stations is shown in Figure 7. We used VELEST single-event mode for computing the parameters. Results for these four earthquakes are shown in Figure 8, for which the variation of rms residual is plotted as a function of depth for different subsets of phase data (all *P* and *S* arrivals, and all *P* arrivals). For these earthquakes, we have robust estimate of depth as the rms versus depth function is sharp around the minimum. The computed value of depth through inversion is shown for individual events. This exercise established the credibility of our located earthquake.

In Figure 9 we indicate the sequence of events from 50 h before to 30 h after a $Mw = 4.4$ earthquake marked at time $t = 0$. To examine how the earthquake initiated at depth, we plot the time–depth section of earthquake occurrence (Figure 9 *a*) for a time-period from 50 h before to 33 h after the main shock. The sequence initiated at a depth of ~6 km. Around 500 min before the main shock, a burst of seismicity is observed across the whole seismogenic depth from 2 to 9 km. Aftershocks are confined largely to a depth of 6–8 km. We note that the deeper seismogenic zone (5–10 km) where the earthquakes initiated is characterized by high strain energy and high stress drop, whereas the shallower level (1–4 km) has low strain energy and low stress drop[12].

To study the nature of spatial migration of earthquakes, we plotted the epicentre distribution along the latitude with time of their occurrence. We observe that the earthquakes occur almost at the same latitude. Just prior to the main shock, in a short time duration (in less than 300 min before the main shock), the earthquakes migrate

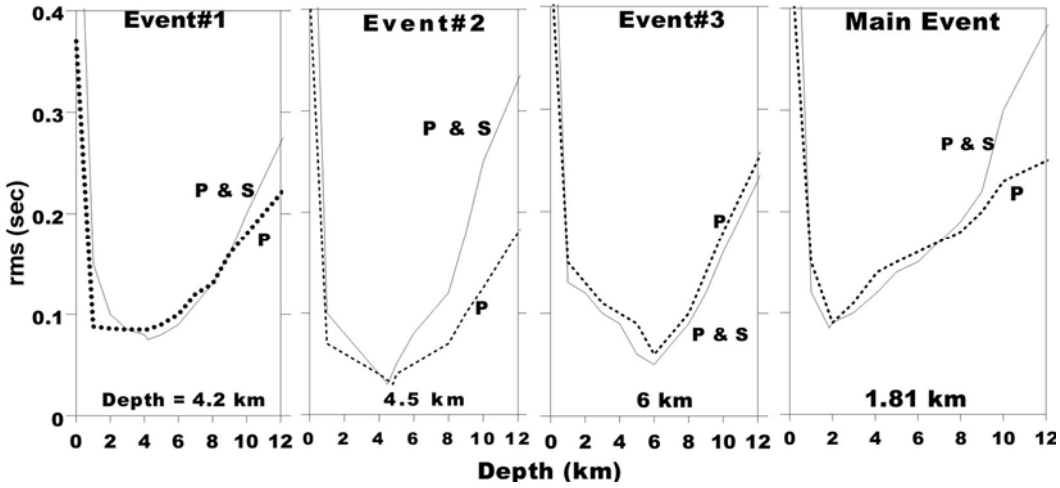

Figure 8. Plot of rms error versus focal deplth for four selected earthquakes (shown in Figure 6) computed using single-event modelling option. Line style indicates the subset of arrival times used for earthquake location: dotted lines, only *P* arrivals; solid lines, *P* and *S* arrivals. Depth computed is similar to that obtained earlier through double-difference inversion.

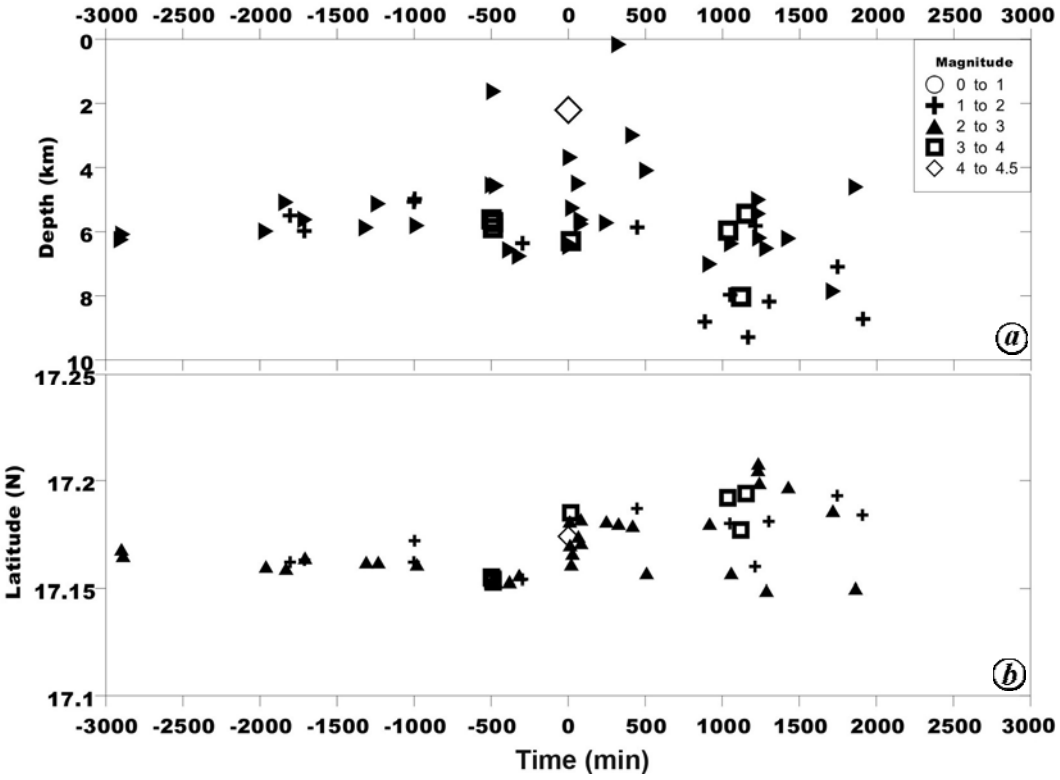

Figure 9. Migration of earthquake sequence with (***a***) depth and (***b***) latitude plotted for the time-period –3000 min (foreshocks) to + 3000 min (aftershocks). 0 time refers to occurrence of main shock.

northward by 3–4 km. This may be interpreted as possible movement from one to another fault system with distinct mechanical property.

We carefully located a foreshock/aftershock sequence that forms the basis of the earthquake nucleation process and serves as a prediction method invoked for use in Koyna region. The method proposed by Mandal *et al.*[2], and Rastogi and Mandal[3] supposes downward propagation of earthquakes. Contrary to this, we find upward shift in micro-earthquake activity from a depth of ~6–8 km and the main earthquake occurring at a depth of only 1.8 km. Our study supports the earlier conclusion of Macelwane[13] that earthquakes nucleate near the base of the seismic zone and not from near the top. This is also

supported by Das and Scholz[5], who used the dynamical model and found that ruptures that initiate in a shallow (low stress) region are prevented from propagating into deeper (high strength) regions. Instead, ruptures that initiate in deeper (high-stress region) are capable of propagating through the entire 'schizosphere'. This view is supported by prediction from friction data coupled with stability analysis[14] that earthquakes should not nucleate within the upper region of mature fault zones[15], i.e. 1–4 km in this case. Assuming that frequency–magnitude statistics can be used to estimate probabilities of a small rupture initiation growing into a larger earthquake, Mori and Abercombie[16] showed that a small (magnitude 2) rupture initiated at a depth of 9–12 km is 18 times more likely to grow into a magnitude 5.5 or larger event compared to the small rupture initiation at shallower depth of 0–3 km. We conclude based on theoretical and experimental considerations, that earthquakes in Koyna region initiate at deeper level and propagate upward along a fault plane surface. These results clearly demonstrate that the earlier proposed hypothesis that earthquakes in Koyna region nucleate at shallow depth and migrate downward is not tenable and hence the earthquake prediction model must be discarded.

The results call for developing a new model for nucleation of earthquakes in Koyna region with better located hypocentres and supported by appropriate dynamical simulation of geo-mechanical systems using accurate description of 3D geometry and mechanical property of the fault systems, hitherto lacking despite over five decades of geophysical investigation in the region.

1. Ohnaka, M., Nonuniformity of the constitutive law parameters for shear rupture and quasistatic nucleation to dynamic rupture: a physical model of earthquake generation processes. *Proc. Natl. Acad. Sci. USA*, 1996, **93**, 3795–3802.
2. Mandal, P. *et al.*, Method of short term forecasting of moderate sized earthquakes. US Patent 2003/0182065 A1, September 2003.
3. Rastogi, B. K. and Mandal, P., Foreshock and nucleation of small to moderate sized Koyna earthquakes (India). *Bull. Seismol. Soc. Am*., 1999, **89**, 829–836.
4. Abercrombie, R. E. and Mori, J., Occurrence, patterns of foreshocks to large earthquakes in the western United States. *Nature*, 1997, **381**, 303–307.
5. Das, S. and Scholz, C. H., Why large earthquakes do not nucleate at shallow depth? *Nature*, 1983, **305**, 621–623.
6. Rai, S. S., Singh, S. K., Sarma, P. V. S. S., Srinagesh, D., Reddy, K. N. S., Prakasam, K. S. and Satyanaryana, Y., What triggers Koyna region earthquakes? Preliminary results from seismic tomography digital array. *Proc. Indian Acad. Sci*. (*Earth Planet. Sci*.), 1999, **108**, 1–14.
7. Kissling, E., Geotomography with local earthquake data. *Rev. Geophys.*, 1988, **26**, 659–698.
8. Waldhauser, F. and Ellsworth, W. L., Double difference location algorithm: method and application to Northern Hayward fault, California. *Bull. Seismol. Soc. Am*., 2000, **90**, 1353–1368.
9. Waldhauser, F., HypoDD – a program to compute double difference hypocenter locations. US Geol. Surv. Open file report, 01-113, 2001, p. 113.
10. Got, J. L., Frechet, J. and Klein, F. W., Deep fault geometry inferred from multiple relative relocations beneath the south flank of Kilauea. *J. Geophys. Res*., 1994, **99**, 15375–15386.
11. Page, C. C. and Saunders, M. A., LSQR: an algorithm for sparse linear equation and sparse least squares. *ACM Trans. Math. Software*, 1982, **8**, 43–71.
12. Mandal, P., Rastogi, B. K. and Sarma, C. S. P., Source parameters of Koyna earthquakes, India. *Bull. Seismol. Soc. Am.*, 1998, **88**, 833–842.
13. Macelwane, J., Problems and progress on the geological–seismological front. *Science*, 1936, **83**, 193–198.
14. Rice, J. R. and Ruina, A. L., Stability of steady and frictional slipping. *J. Appl. Mech*., 1983, **105**, 343–349.
15. Marone, C. and Scholz, C. H., The depth of seismic faulting and the upper transition from stable to unstable slip regimes. *Geophys. Res. Lett*., 1988, **15**, 621–624.
16. Mori, J. and Abercrombie, R. E., Depth dependence of earthquake frequency–magnitude distribution in California. Implication of rupture initiation. *J. Geophys. Res*., 1997, **102**, 15081–15090.

ACKNOWLEDGEMENTS. S.S.R. is supported by J.C. Bose Fellowship from DST, New Delhi. Field observation was supported by a research project from DST. We thank the anonymous reviewer for critical suggestions that helped improve the manuscript.

Received 5 August 2013; revised accepted 24 September 2013

Early to Middle Albian age calcareous nannofossils from Pariwar Formation of Jaisalmer Basin, Rajasthan, western India and their significance

Jyotsana Rai[1,*], Abha Singh[1] and Dhirendra Kumar Pandey[2]

[1]Birbal Sahni Institute of Palaeobotany, 53, University Road, Lucknow 226 007, India
[2]University of Rajasthan, Jaipur 302 004, India

Early–Middle Albian calcareous nannofossil assemblage comprising 55 species has been recovered from the Pariwar Formation, Jaisalmer Basin, western India. The nannofossils are moderate to well-preserved and are calibrated with Early–Middle nannofossil zones CC7–CC8 of Albian age. The present record of nannofossils indicates a marine depositional environment with good connection to the open ocean for the Pariwar Formation. Presence of species, *Seribiscutum primitivum* in small numbers in surface sediments of Pariwar Formation and its common occurrence in coeval subsurface succession of Tanot Well-1 is the first record from the Cretaceous of Western India, which was located at ~30°S of the equator during mid-Cretaceous. *S. primitivum* is considered as cold-water, high-latitude taxa. Its presence in the Jaisalmer Basin

*For correspondence. (e-mail: jyotsana_rai@yahoo.com)